NLO SUSY pair production in MadGOLEM

2nd IMPRS seminar

November 18 2011 Heidelberg

PT FS FOR PRECISION TESTS OF FUNDAMENTAL SYMMETRIES

Dorival Gonçalves-Netto

collaborators D. Lopez-Val, T. Plehn, K. Mawatari, I. Wigmore

ITP - Universität Heidelberg

Institut für Theoretische Physik

Ruprecht-Karls Universität Heidelberg

Outline

- Motivations
- Perturbative (SUSY-)QCD
  - Structure of the NLO corrections
  - Catani-Seymour Subtraction Method
  - MadGOLEM
- One major LHC search channel: SUSY Monojet signatures
  - NLO corrections
  - Pheno analysis
- Summary

Motivations

- Why Next-to-Leading order (NLO)?
  - Less sensibility from unphysical factorization/renormalization scales

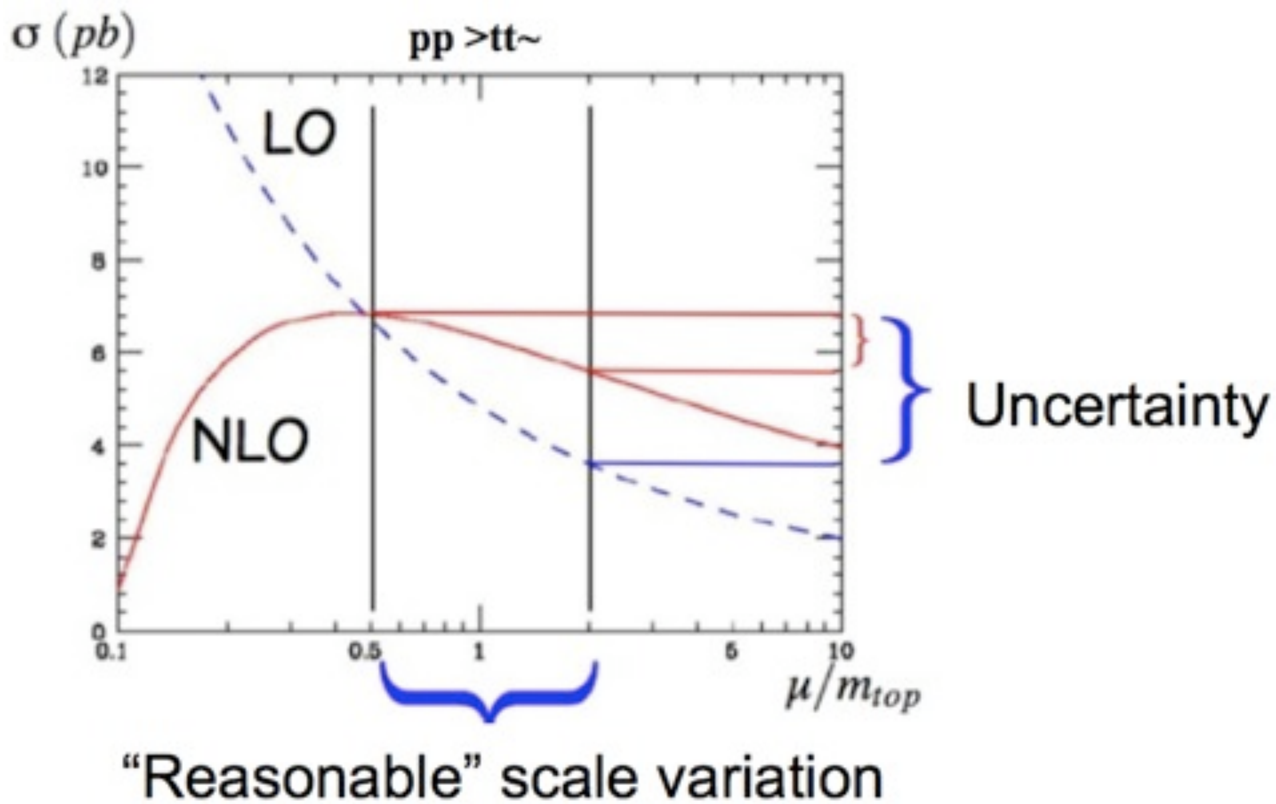

  - Improve shape of distributions
  - New channels & kinematics arising from NLO can have a high impact (particularly in the presence of cuts)
  - Not yet fully automated

Motivations

- PROSPINO (PROduction of Supersymmetric Particles in Next-to-leading Order) [Beenakker, Höpker, Krämer, Plehn, Spira, Zerwas]

➡ The only public available code to do SUSY NLO cross sections

➡ It's hard coded, process dependent

➡ Just gives total cross sections (no distributions).

- MadGOLEM: Fully automated tool to perform NLO QCD for BSM (main focus on SUSY models)

➡ Process independent

➡ Gives total cross sections and distributions

➡ Allow the user to apply cuts...

Motivations

- SUSY pair production at the LHC:

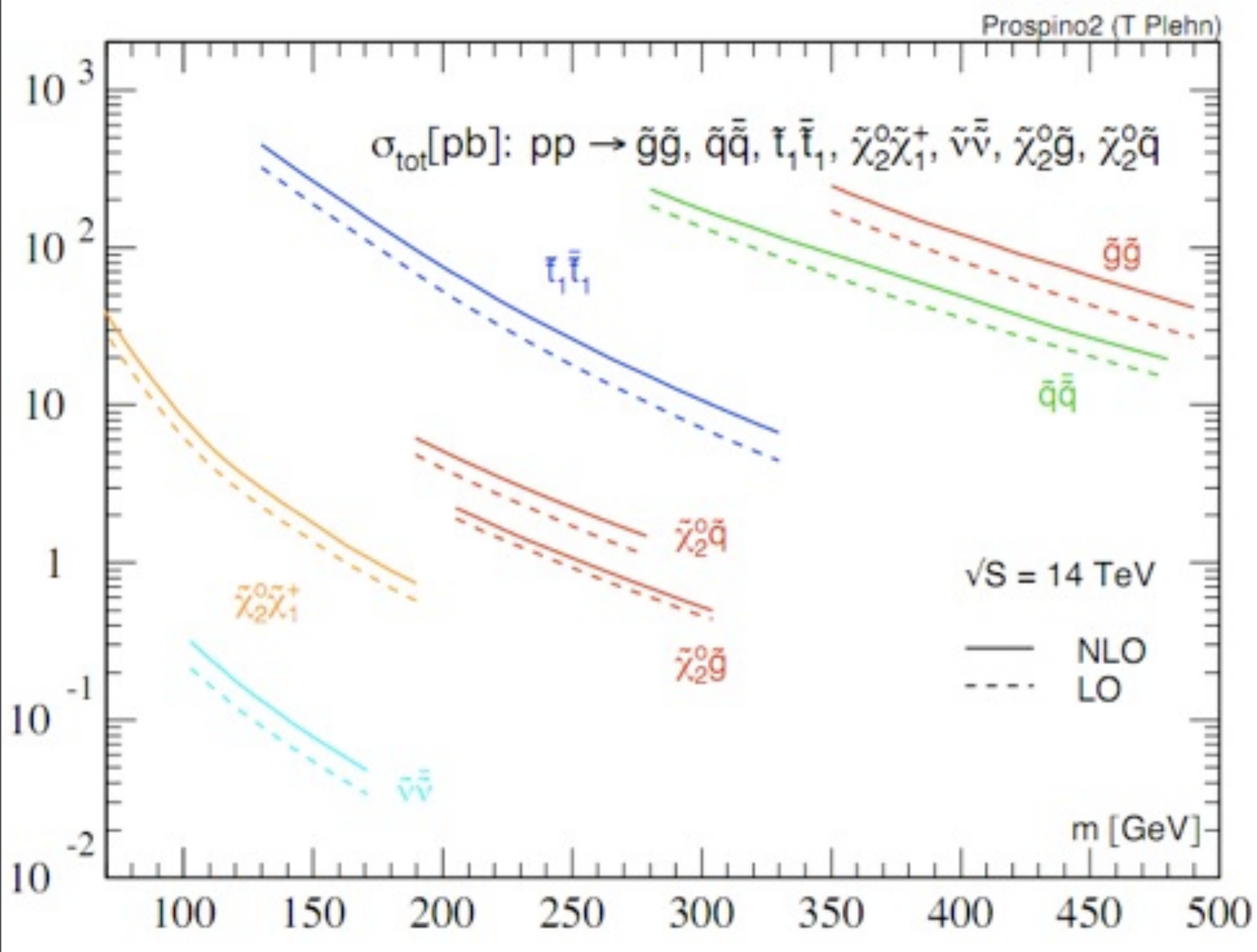

$$K = \frac{\sigma^{NLO}}{\sigma^{LO}} \sim 1.3 - 1.5$$

NLO correction quantitatively relevant!

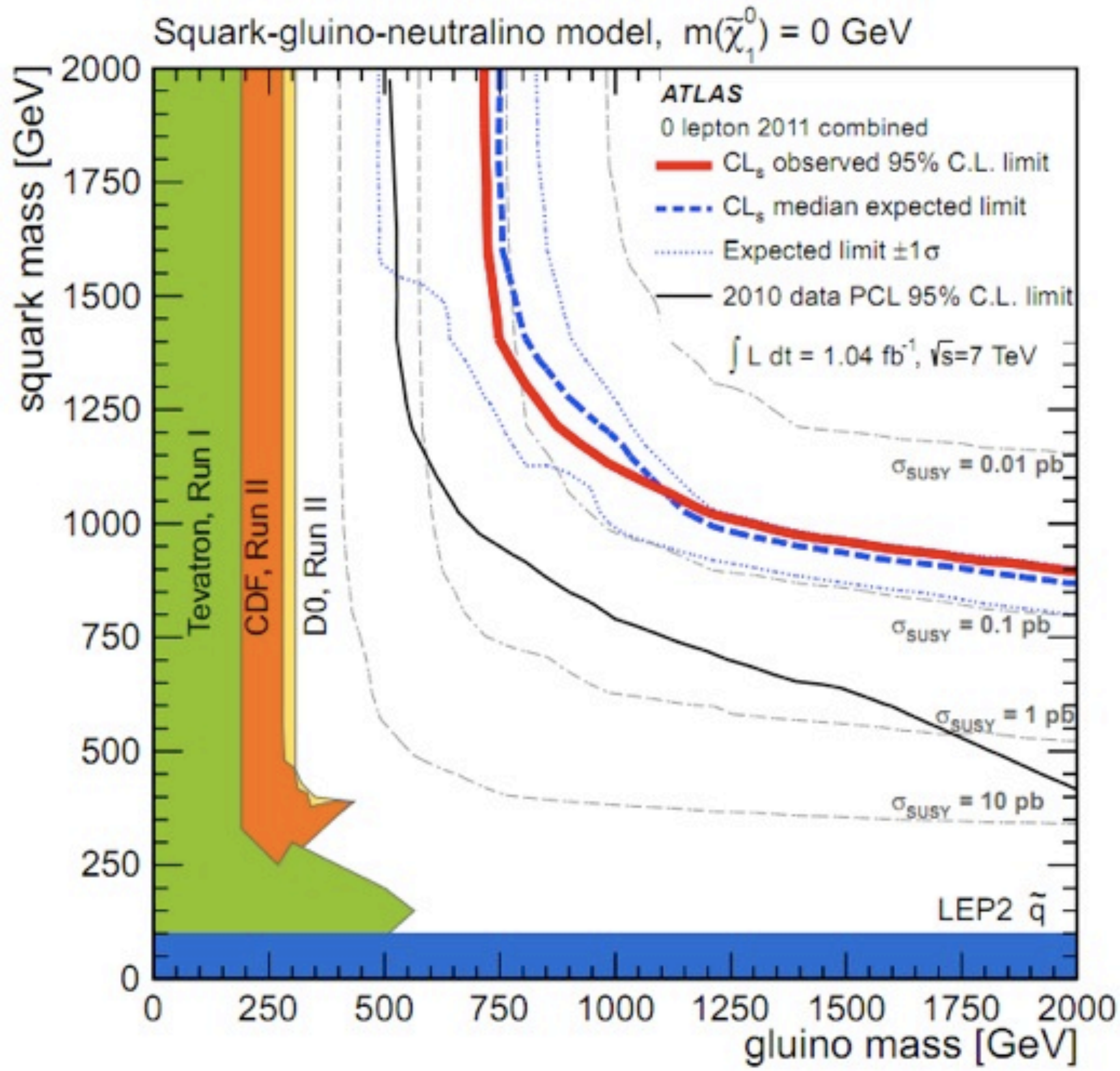

"SUSY signal samples are generated with HERWIG++, normalized using the NLO cross section determined by PROSPINO." [1109.6572[hep-ex]]

Perturbative QCD

- Master Formula: Factorizes the hard and soft processes.

$$\sigma_{pp\to X} = \sum_{i,j,\{k\}} \int dx_1 dx_2 f_i(x_1) f_j(x_2) \hat{\sigma}_{ij\to\{k\}}(\alpha_s, Q) \otimes D_{\{k\}\to X}$$

Parton distribution function (Non-perturbative)

Subprocess partonic cross section (Perturbative)

Jet algorithm
Parton shower
Hadronization model

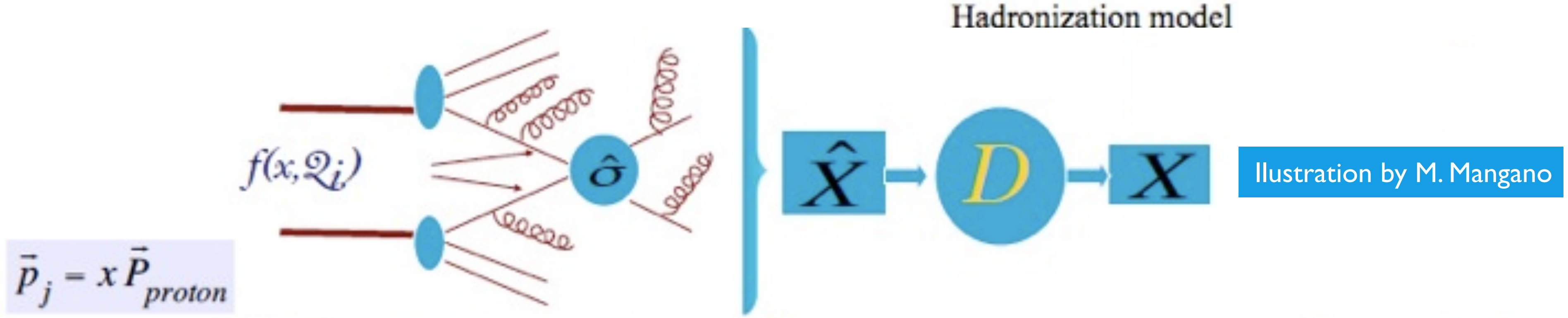

$f_a(x_a, Q_i^2)$ Parton distribution functions (PDF)

$D(\hat{X}_f \to X, Q_i^2, Q_f^2)$ Fragmentation Function (FF)

Perturbative expansion from the partonic cross section:

$$\hat{\sigma}_{ab\to f} = \sigma_0 + \alpha_s \sigma_1 + \alpha_s^2 \sigma_2 + \ldots$$

Leading Order

Next-to-Leading Order

Next-to-Next-to-Leading Order

Structure of the NLO corrections

$$\delta\sigma^{NLO} = \int_{n+1} d\sigma^{Real} + \int_n d\sigma^{Collinear} + \int_n d\sigma^{Virtual}$$

Real emission
Born matrix with n+1 partons

IR divergent

Collinear subtraction
From factorization of initial state collinear singularities

IR divergent

Virtual corrections
Interference term of 1-loop & Born matrix

IR divergent

UV divergent → Renormalization → UV finite

Structure of the NLO corrections

$$\delta\sigma^{NLO} = \int_{n+1} d\sigma^{Real} + \int_n d\sigma^{Collinear} + \int_n d\sigma^{Virtual}$$

Real emission
Born matrix with n+1 partons

Collinear subtraction
From factorization of initial state collinear singularities

Virtual corrections
Interference term of 1-loop & Born matrix

UV divergent → Renormalization → UV finite

IR divergent + IR divergent + IR divergent

→ Finite and IR safe
(KLN & Factorization Theorem)

Problems:

- Analytic integration in d dimensions only feasible for very simple fully inclusive processes
- How to get individual contributions finite via MC methods?

Structure of the NLO corrections

- **Subtraction Method** (Warm up):

$$\int_0^1 \frac{F(x)}{x^{1-\varepsilon}}dx = \int_0^1 \frac{F(x)-F(0)}{x^{1-\varepsilon}}dx + \int_0^1 \frac{F(0)}{x^{1-\varepsilon}}dx$$
$$= \int_0^1 \frac{F(x)-F(0)}{x}dx + \frac{F(0)}{\varepsilon}$$

- **Catani-Seymour Subtraction Method**: construction of local counter terms using the universality of soft and collinear limits

$$|\mathcal{M}_{n+1}|^2 \to |\mathcal{M}_n|^2 \otimes V_{ij,k} \quad \Longrightarrow \quad d\sigma^A \equiv \sum_{dipoles} d\sigma^B \otimes dV_{dipole}$$

$$\delta\sigma^{NLO} = \int_{n+1}\left(d\sigma^{Real}_{\varepsilon=0} - d\sigma^{A}_{\varepsilon=0}\right) + \int_n \left(d\sigma^{Collinear} + d\sigma^{Virtual} + \int_1 d\sigma^A\right)_{\varepsilon=0}$$

- Vij,k is a singular factor, and depends only on the quantum numbers of i, j and k, and on their momenta. It is completely process independent.

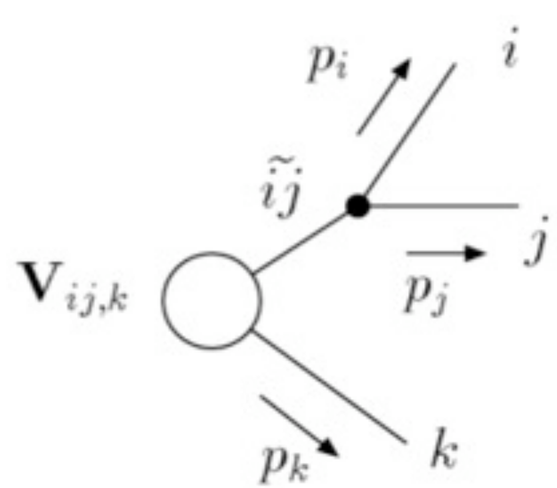

Structure of the NLO corrections

- Subtraction Method (Warm up):

$$\int_0^1 \frac{F(x)}{x^{1-\varepsilon}}dx = \int_0^1 \frac{F(x)-F(0)}{x^{1-\varepsilon}}dx + \int_0^1 \frac{F(0)}{x^{1-\varepsilon}}dx$$
$$= \int_0^1 \frac{F(x)-F(0)}{x}dx + \frac{F(0)}{\varepsilon}$$

- Catani-Seymour Subtraction Method: construction of local counter terms using the universality of soft and collinear limits

$$|\mathcal{M}_{n+1}|^2 \rightarrow |\mathcal{M}_n|^2 \otimes V_{ij,k} \quad \Longrightarrow \quad d\sigma^A \equiv \sum_{dipoles} d\sigma^B \otimes dV_{dipole}$$

$$\delta\sigma^{NLO} = \int_{n+1}\left(d\sigma^{Real}_{\varepsilon=0} - d\sigma^A_{\varepsilon=0}\right) + \int_n \left(d\sigma^{Collinear} + d\sigma^{Virtual} + \int_1 d\sigma^A\right)_{\varepsilon=0}$$

- The Virtual part can be integrable in 4D just after cancelation of the poles, where their pole counter part come from the integrated dipoles

$$\left(\frac{c_2}{\epsilon_{IR}^2} + \frac{c_1}{\epsilon_{IR}} + c_0\right) + \left(\frac{c_2'}{\epsilon_{IR}^2} + \frac{c_1'}{\epsilon_{IR}} + c_0'\right) = c_0 + c_0'$$

Structure of the NLO corrections

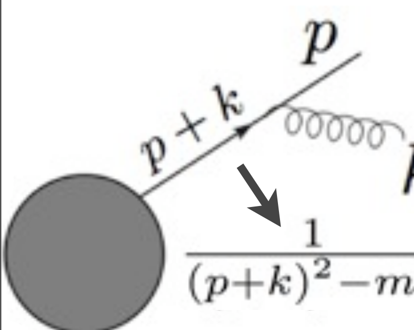

$$\frac{1}{(p+k)^2-m^2} = \frac{1}{2E_k E_p(1-\beta\cos\theta_{kp})}$$

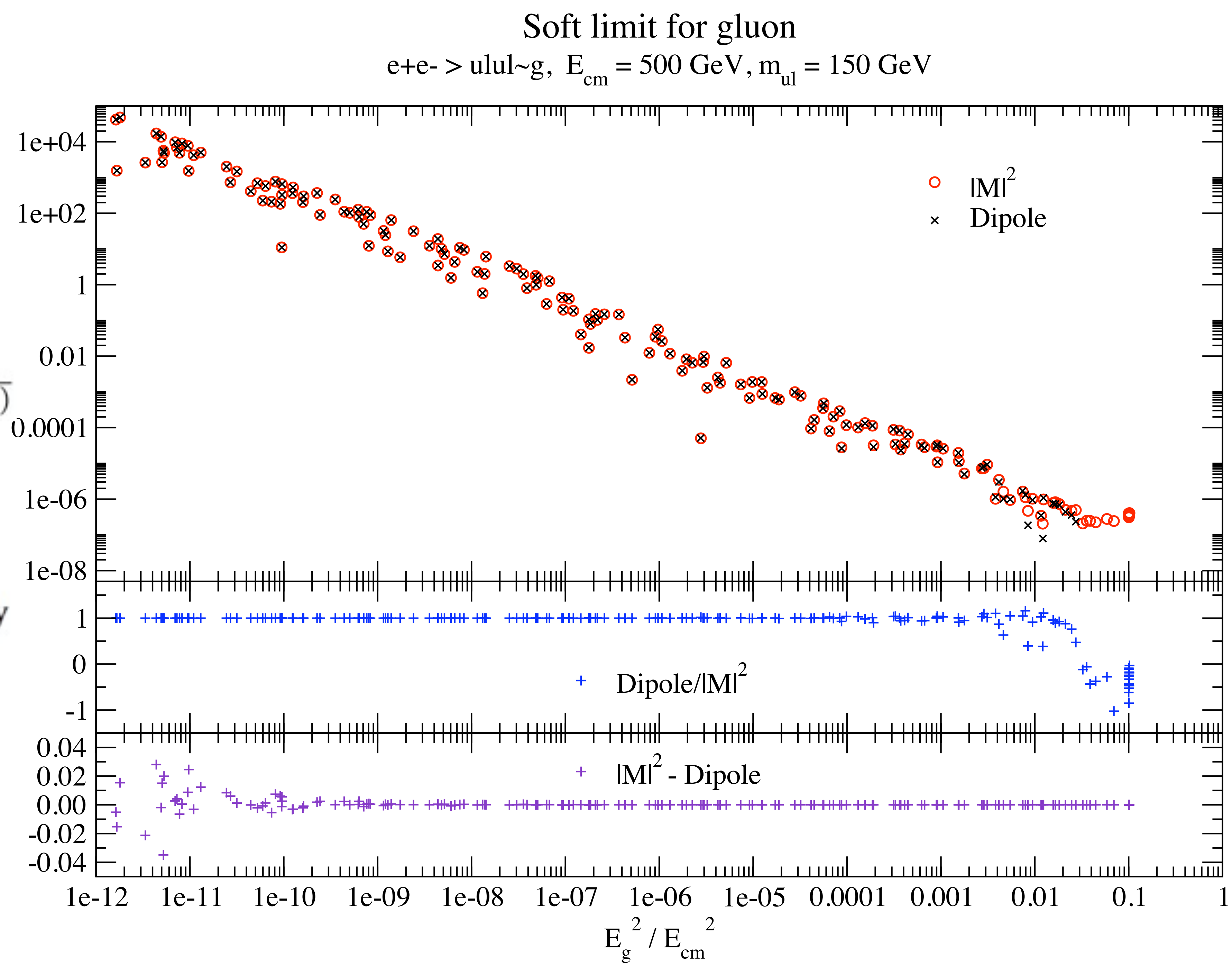

- Soft limit $E_k \to 0$: Soft singularity
- Collinear limit $\theta_{kq} \to 0$: Collinear singularity

$$\delta\sigma^{NLO} = \int_{n+1}\left(d\sigma^{Real}_{\epsilon=0} - d\sigma^{A}_{\epsilon=0}\right) + \int_{n}\left(d\sigma^{Collinear} + d\sigma^{Virtual} + \int_1 d\sigma^{A}\right)_{\epsilon=0}$$

MadGOLEM

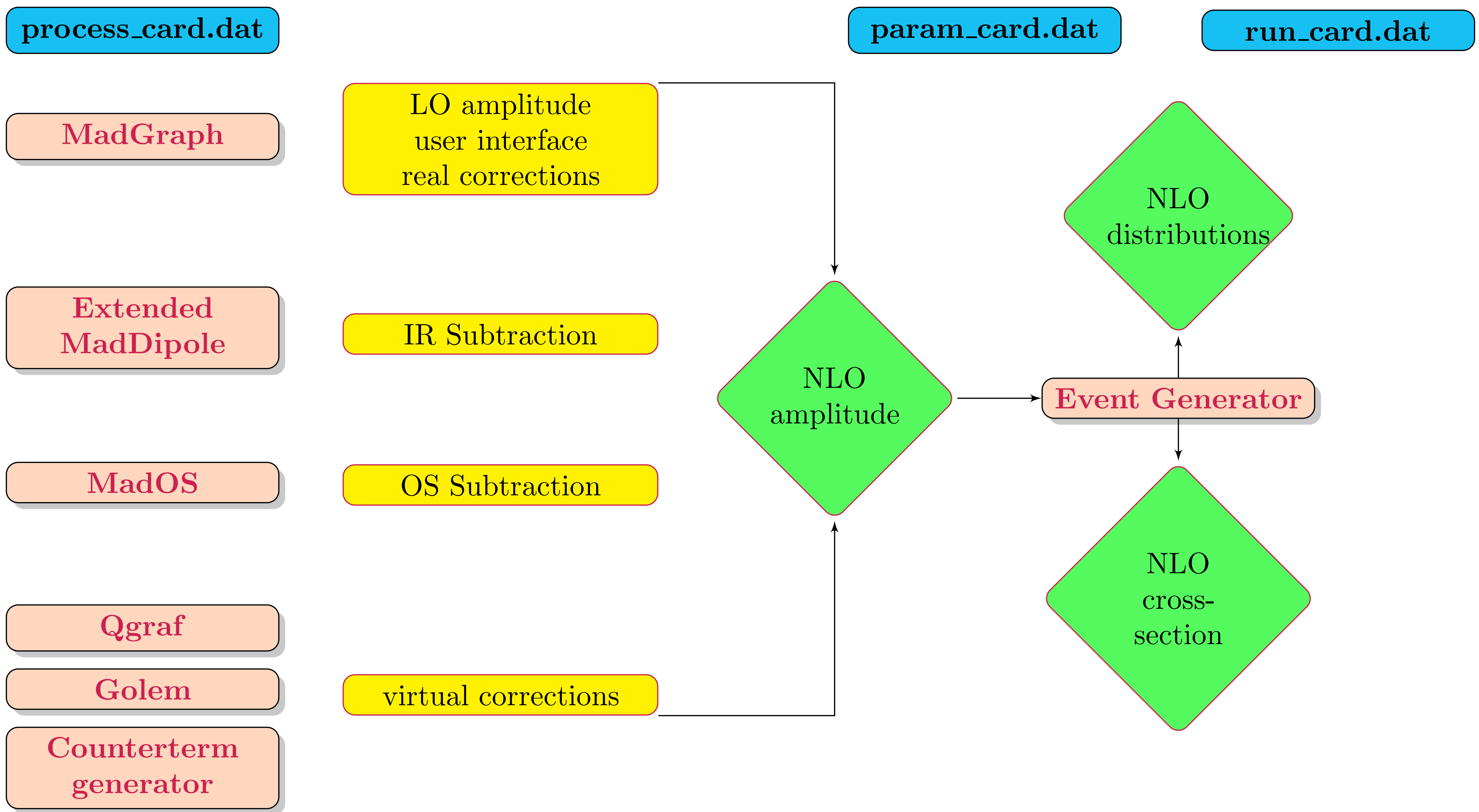

$$\sigma^{NLO} = \int_n d\sigma^{LO} + \int_{n+1} \left(d\sigma^{Real}_{\varepsilon=0} - d\sigma^{A}_{\varepsilon=0} - d\sigma^{OS}_{\varepsilon=0}\right) + \int_n \left(d\sigma^{Virtual} + \int_1 d\sigma^{A}\right)_{\varepsilon=0}$$

DGN, D. Lopez-Val, T. Plehn, K. Mawatari, I. Wigmore

MadGOLEM

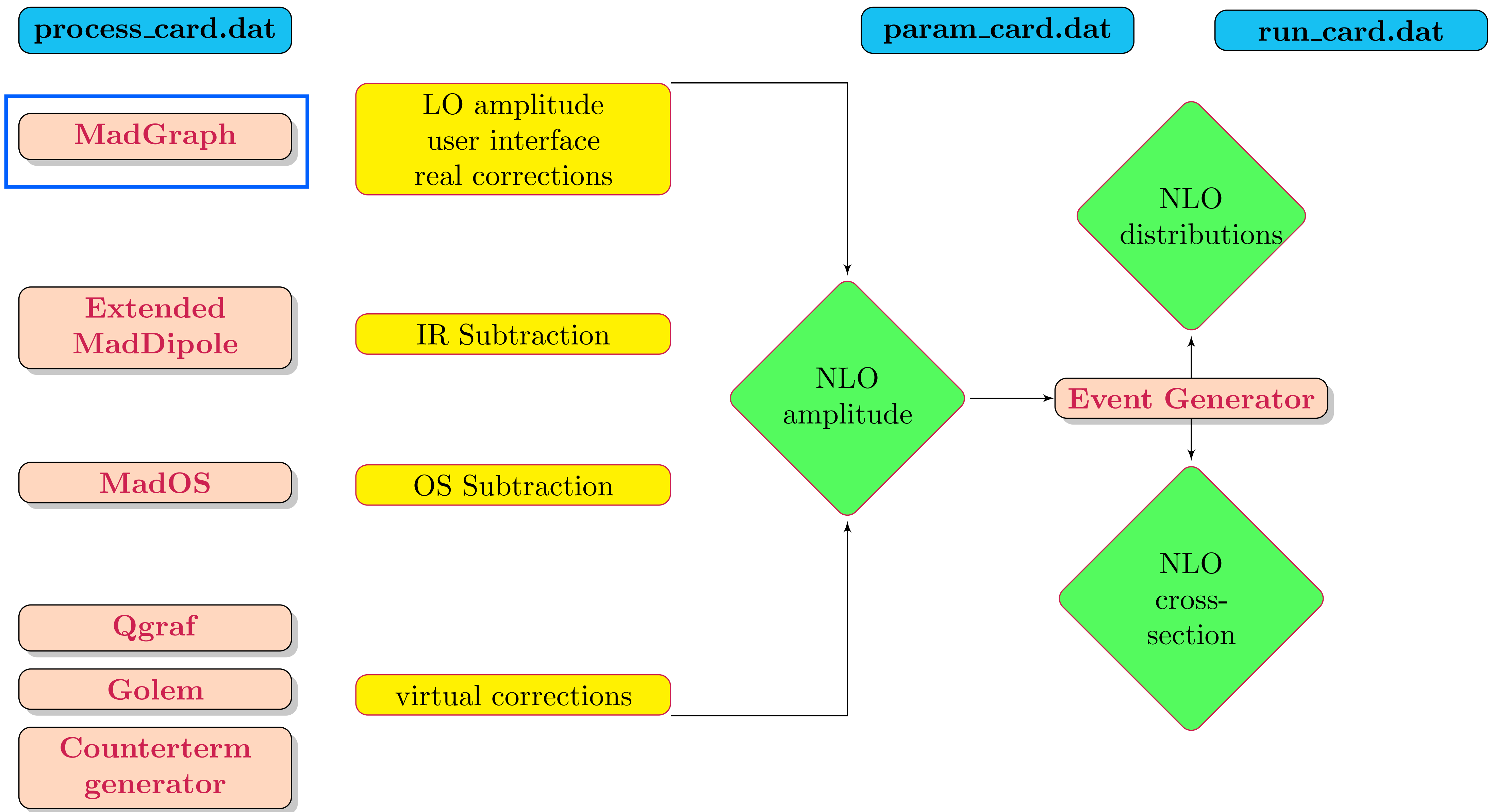

$$\sigma^{NLO} = \int_n d\sigma^{LO} + \int_{n+1} \left(d\sigma^{Real}_{\varepsilon=0} - d\sigma^{A}_{\varepsilon=0} - d\sigma^{OS}_{\varepsilon=0} \right) + \int_n \left(d\sigma^{Virtual} + \int_1 d\sigma^{A} \right)_{\varepsilon=0}$$

DGN, D. Lopez-Val, T. Plehn, K. Mawatari, I. Wigmore

MadGOLEM

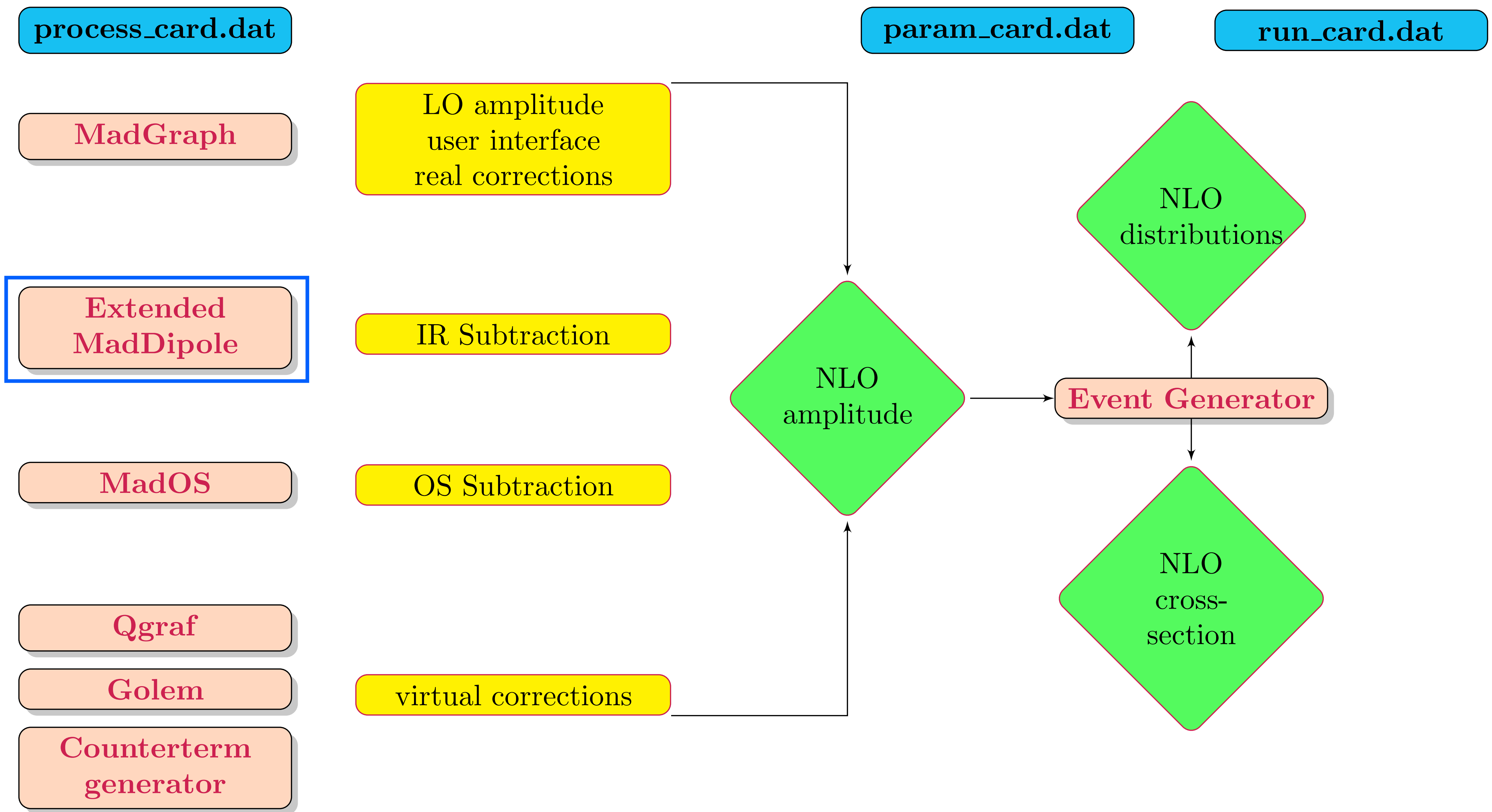

$$\sigma^{NLO} = \int_n d\sigma^{LO} + \int_{n+1} \left(d\sigma^{Real}_{\varepsilon=0} - \boxed{d\sigma^{A}_{\varepsilon=0}} - d\sigma^{OS}_{\varepsilon=0}\right) + \int_n \left(d\sigma^{Virtual} + \boxed{\int_1 d\sigma^{A}}\right)_{\varepsilon=0}$$

DGN, D. Lopez-Val, T. Plehn, K. Mawatari, I. Wigmore

MadGOLEM

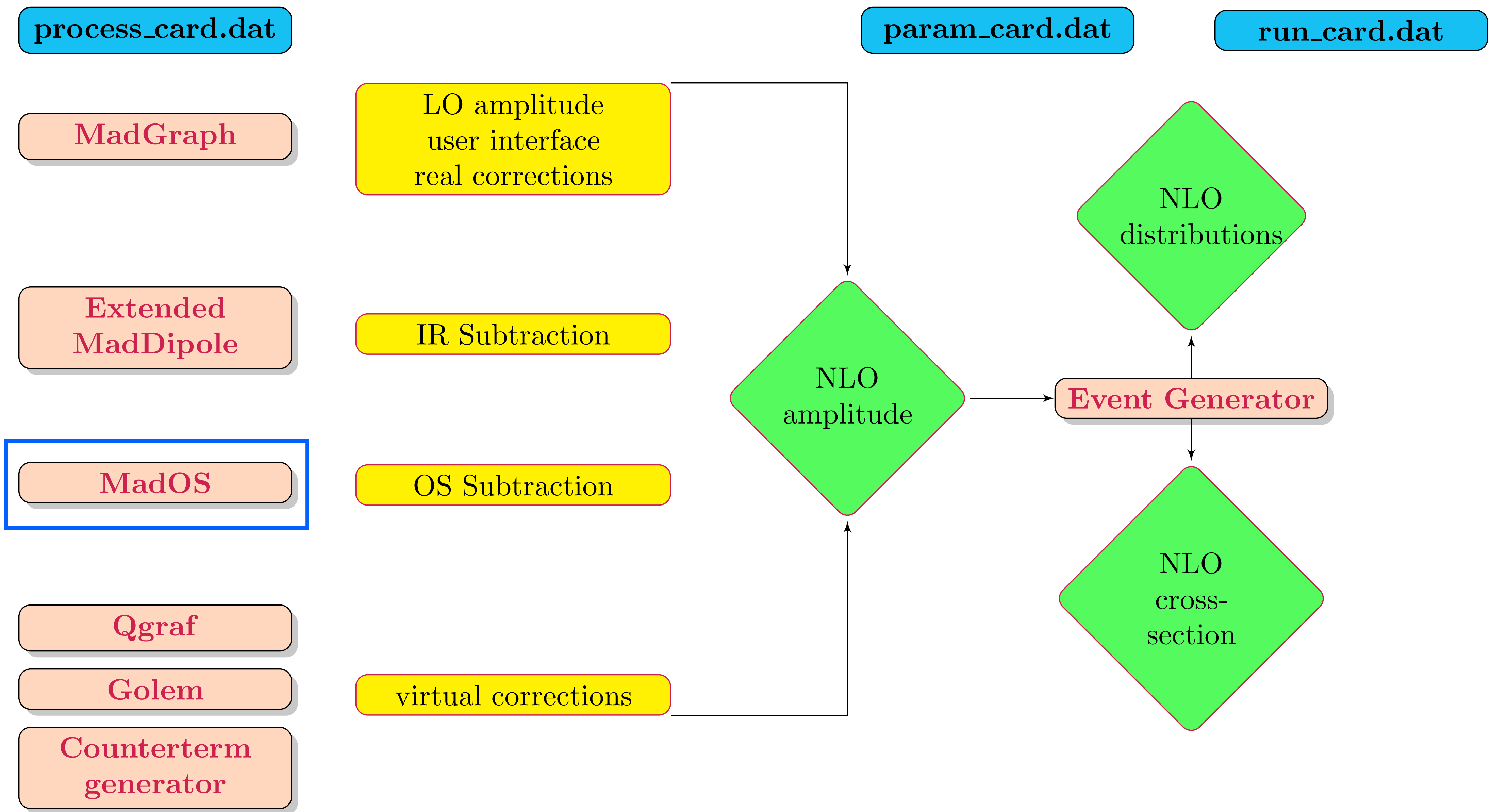

$$\sigma^{NLO} = \int_n d\sigma^{LO} + \int_{n+1} \left(d\sigma^{Real}_{\varepsilon=0} - d\sigma^{A}_{\varepsilon=0} - d\sigma^{OS}_{\varepsilon=0} \right) + \int_n \left(d\sigma^{Virtual} + \int_1 d\sigma^{A} \right)_{\varepsilon=0}$$

DGN, D. Lopez-Val, T. Plehn, K. Mawatari, I. Wigmore

MadGOLEM

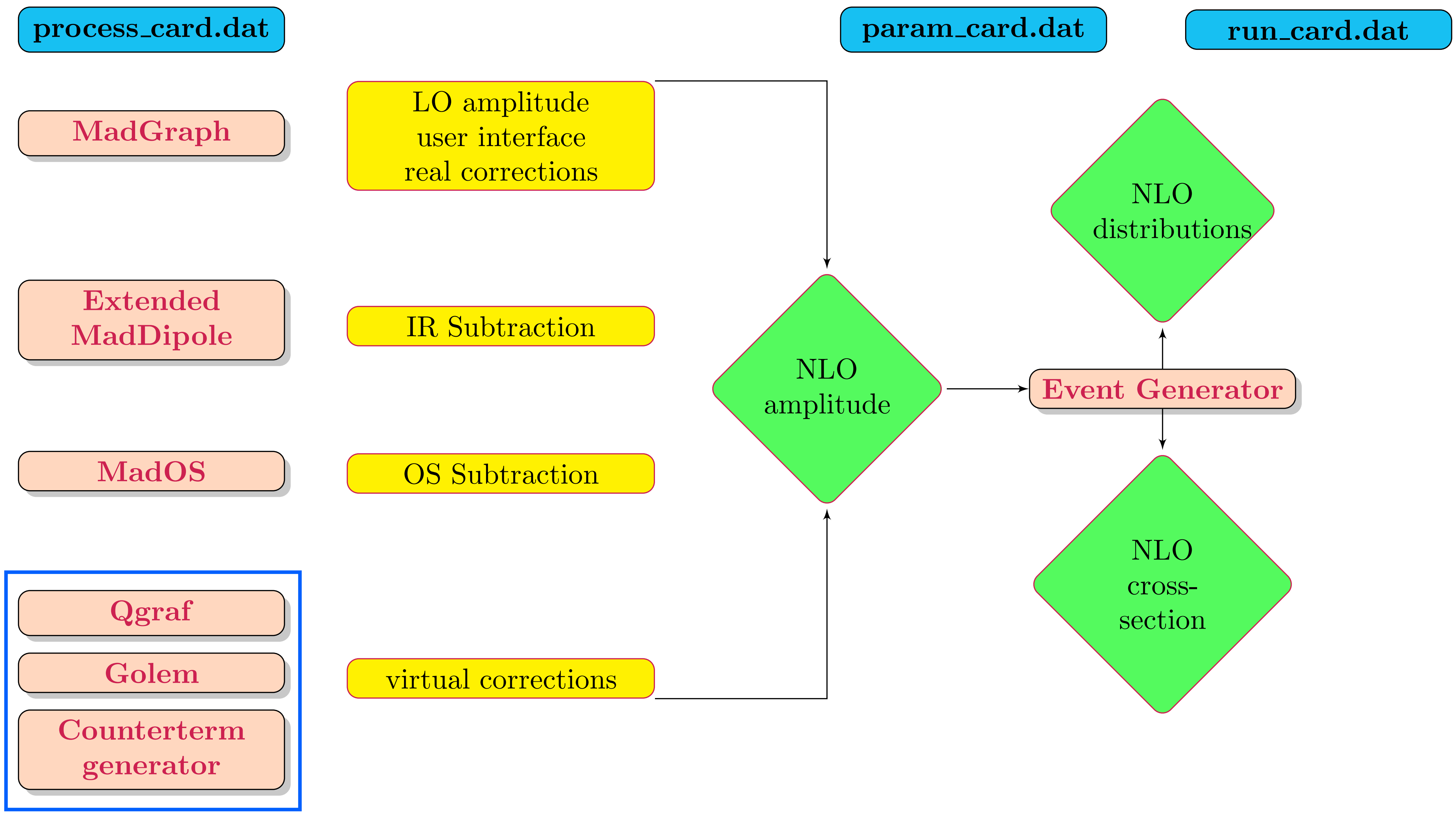

$$\sigma^{NLO} = \int_n d\sigma^{LO} + \int_{n+1} \left(d\sigma^{Real}_{\varepsilon=0} - d\sigma^{A}_{\varepsilon=0} - d\sigma^{OS}_{\varepsilon=0}\right) + \int_n \left(d\sigma^{Virtual} + \int_1 d\sigma^{A}\right)_{\varepsilon=0}$$

DGN, D. Lopez-Val, T. Plehn, K. Mawatari, I. Wigmore

Squark-neutralino at NLO

- For SUSY there are 3 main production modes at the LHC:
  $pp \to \tilde{q}\tilde{q},\ \tilde{q}\tilde{g},\ \tilde{g}\tilde{g}$ (mediated by strong interactions)

➡ though hard to extract any model parameters beyond masses of new particles

interactions determined by gauge symmetry and SUSY, e.g.

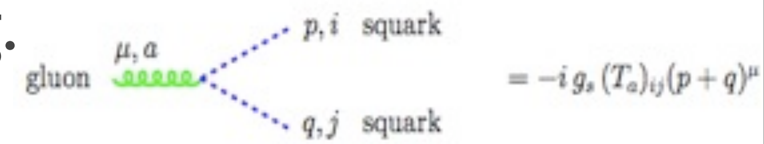

- Important to study production process involving the weakly interacting sector

$pp \to \tilde{q}\tilde{\chi}$ =

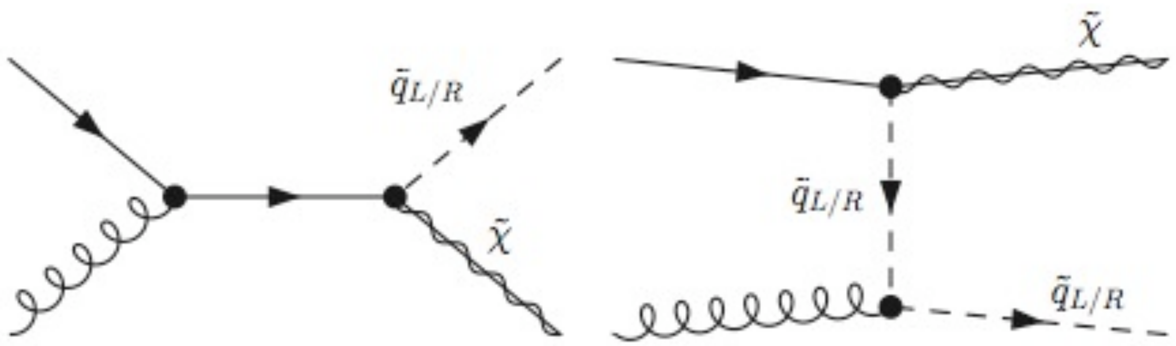

Source of monojet+$\not{E}_T$ signatures

- One hard jet in association + $\not{E}_T$ is one major LHC search channel for BSM

- Associated production: semi-weak process, but favored by $m_{\tilde{\chi}_1^0} \ll m_{\tilde{q}},\ m_{\tilde{g}}$

Squark-neutralino at NLO

- Flavor-locked & semi-weak process sensitive to $q\tilde{q}\tilde{\chi}_1$ coupling: $\sigma^{LO} \sim \mathcal{O}\left(\alpha_{EW}\alpha_s\right)$

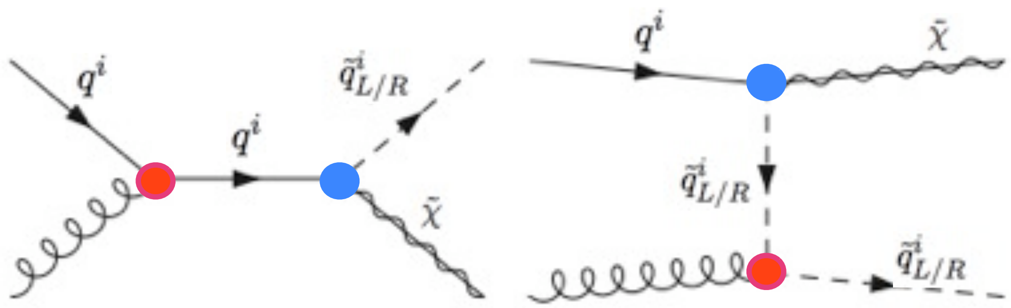

Squark-neutralino at NLO

- Flavor-locked & semi-weak process sensitive to $q\tilde{q}\tilde{\chi}_1$ coupling: $\sigma^{LO} \sim \mathcal{O}\left(\alpha_{EW}\alpha_s\right)$

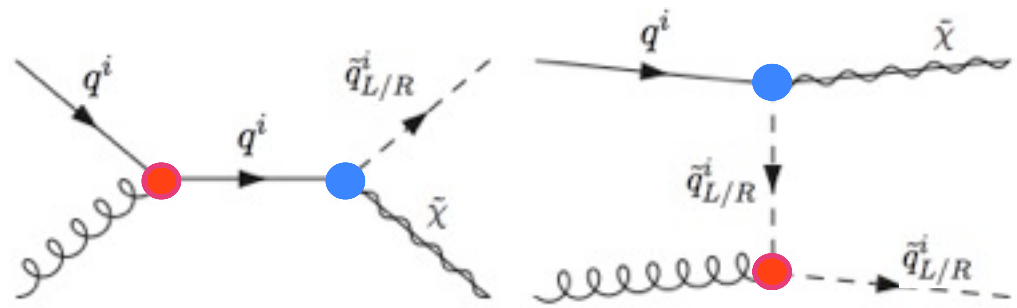

- Couplings size correlated with SUSY breaking:

$$\mathcal{L}_{\tilde{N}_{mass}} = -\frac{1}{2}\left(\psi^0\right)^T \mathbf{M}_{\tilde{N}}\psi^0 + c.c.$$

$$\psi^0 = (\widetilde{B}, \widetilde{W}^0, \widetilde{H}^0_d, \widetilde{H}^0_u)$$

$$\mathbf{N}^*\mathbf{M}_{\tilde{\mathbf{N}}}\mathbf{N}^{-1} = \mathrm{diag}\left(m_{\tilde{\chi}^0_1},\ m_{\tilde{\chi}^0_2},\ m_{\tilde{\chi}^0_3},\ m_{\tilde{\chi}^0_4}\right)$$

$$\mathbf{M}_{\tilde{N}} = \begin{pmatrix} M_1 & 0 & -c_\beta\, s_W\, m_Z & s_\beta\, s_W\, m_Z \\ 0 & M_2 & c_\beta\, c_W\, m_Z & -s_\beta\, c_W\, m_Z \\ -c_\beta\, s_W\, m_Z & c_\beta\, c_W\, m_Z & 0 & -\mu \\ s_\beta\, s_W\, m_Z & -s_\beta\, c_W\, m_Z & -\mu & 0 \end{pmatrix}$$

- Msugra models (SPS1-6): typically give $m_Z \lesssim |M_1| \simeq \frac{1}{2}|M_2| \ll |\mu|$

$\tilde{\chi}^0_1 \simeq \tilde{B}$ (Bino like) e.g. SPS1a $\sigma^{LO}\left(\tilde{u}_R\tilde{\chi}^0_1\right) \gg \sigma^{LO}\left(\tilde{u}_L\tilde{\chi}^0_1\right)$, $\frac{g_{u\tilde{u}_L\tilde{\chi}^0_1}}{g_{u\tilde{u}_R\tilde{\chi}^0_1}} \approx \frac{1}{6}$

- Anomaly mediation (SPS9): $M_1 = \frac{F_\phi}{16\pi^2}\frac{33}{5}g_1^2;\ M_2 = \frac{F_\phi}{16\pi^2}g_2^2 \ \Rightarrow |M_2| \ll |M_1|$

$\tilde{\chi}^0_1 \simeq \tilde{W}$ (Wino like)

Squark-neutralino at NLO

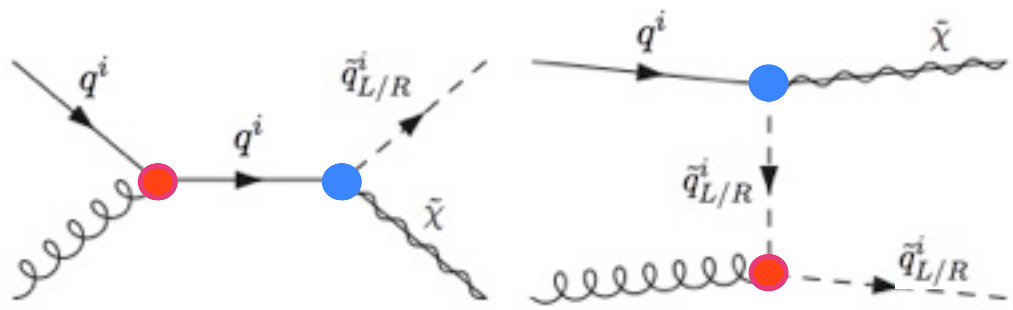

- Provides information on $q\tilde{q}\tilde{\chi}_1$ coupling
  - Reveals the nature of the LSP (bino or wino-like)
  - Bino (wino) coupling proportional to g' (g)
  - Extra info on this coupling would help DM direct detection bounds
- Recent analysis @LO [Allanach, Grab, Haber arXiv:1010.4261]
  Process not yet studied @NLO!
- QCD corrections are quantitatively relevant and important to reduce scale dependence and normalize distributions
- First application of MadGOLEM

Structure of the NLO corrections

- **Real emission** diagrams $pp \to \tilde{q}\tilde{\chi}_1 j$: quark or gluon emission

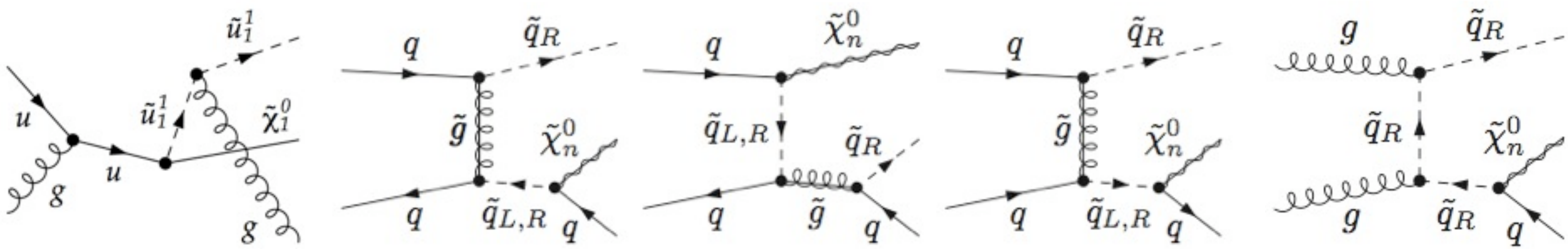

→ Need Catani-Seymour SUSY dipoles

→ On-Shell Subtraction Method to avoid double counting

Structure of the NLO corrections

- **Real emission** diagrams $pp \to \tilde{q}\tilde{\chi}_1 j$: quark or gluon emission

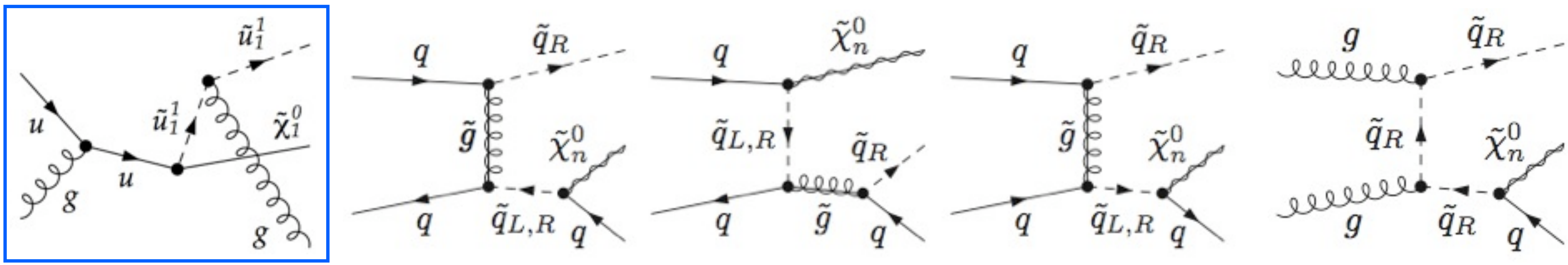

→ Need Catani-Seymour SUSY dipoles

→ On-Shell Subtraction Method to avoid double counting

Structure of the NLO corrections

- **Real emission** diagrams $pp \to \tilde{q}\tilde{\chi}_1 j$: quark or gluon emission

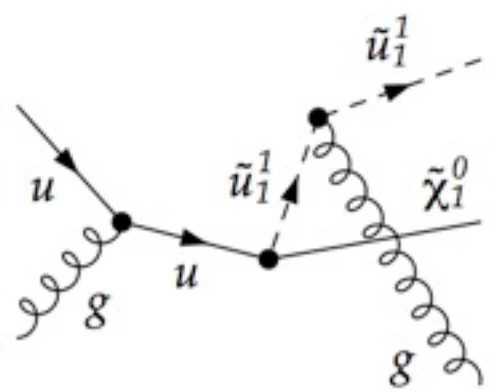

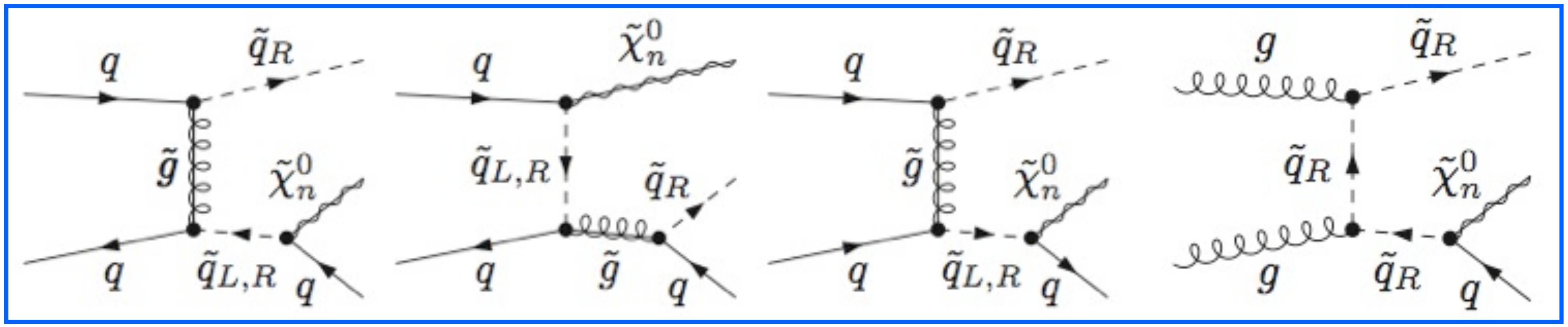

→ Need Catani-Seymour SUSY dipoles

→ On-Shell Subtraction Method to avoid double counting

Structure of the NLO corrections

- On-shell subtraction method: differentiation between off & on-shell production to avoid double counting [Beenakker, Hopker, Spira, Zerwas '97] (Prospino scheme)

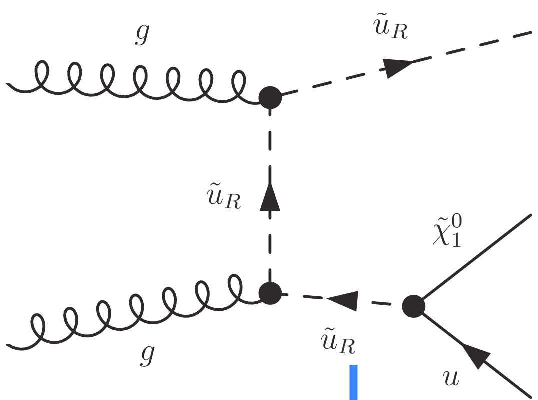

- $gg \to \tilde{q}\bar{\tilde{q}}^* \to \tilde{q}\chi_1\bar{q}$ squark neutralino production
- $gg \to \tilde{q}\bar{\tilde{q}} * BR(\bar{\tilde{q}} \to \chi_1\bar{q})$ squark pair production

$$\frac{i}{p^2 - m_{os}^2} \to \frac{i}{p^2 - m_{os}^2 + i m_{os}\Gamma_{os}}$$

Γ_{OS} is regarded as a regulator

- To avoid double counting subtract on-shell amplitudes:

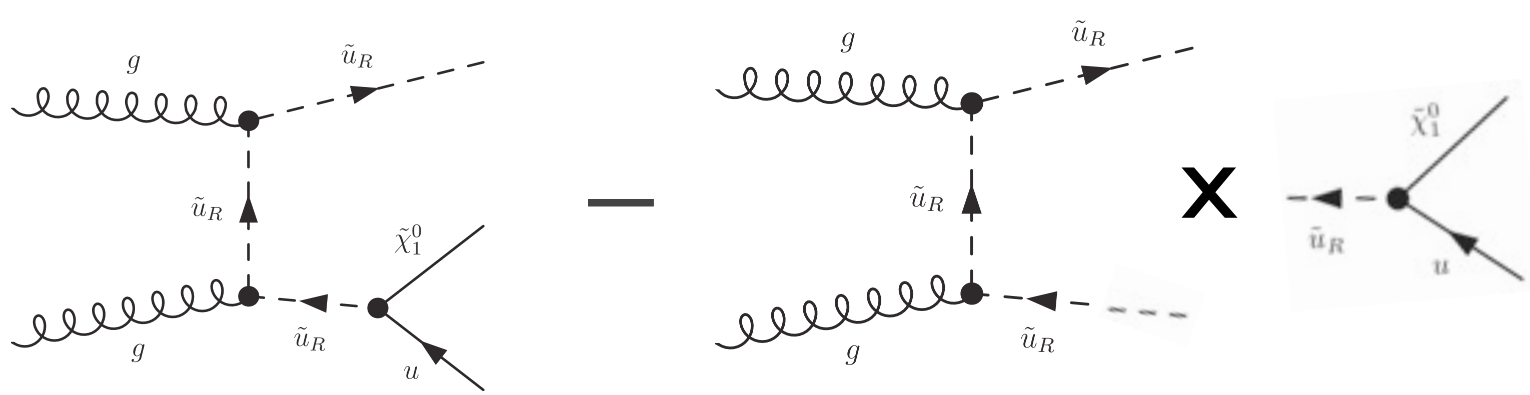

$$\sigma(gg \to \tilde{q}\chi_1\bar{q}) \qquad \sigma(gg \to \tilde{q}\bar{\tilde{q}}) * BR(\bar{\tilde{q}} \to \chi_1\bar{q})$$

Structure of the NLO corrections

- **Virtual** QCD and SUSY-QCD corrections:

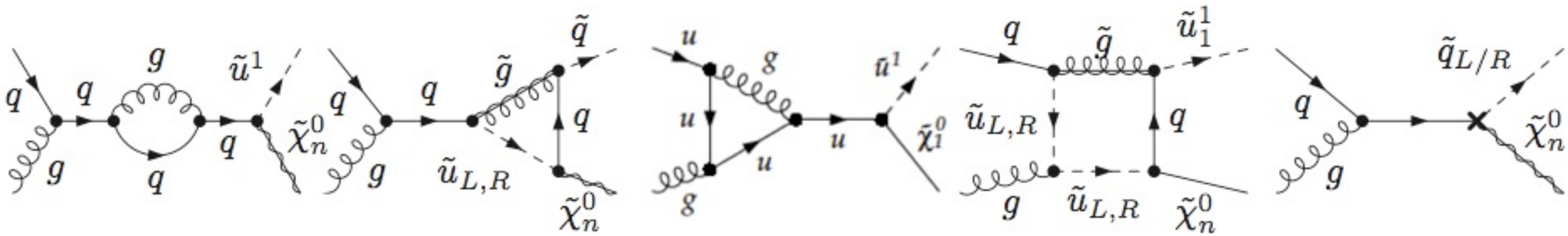

- a) self energy corrections; b) vertex corrections; c) box diagrams; d) UV counter terms

Structure of the NLO corrections

- **Virtual** QCD and SUSY-QCD corrections:

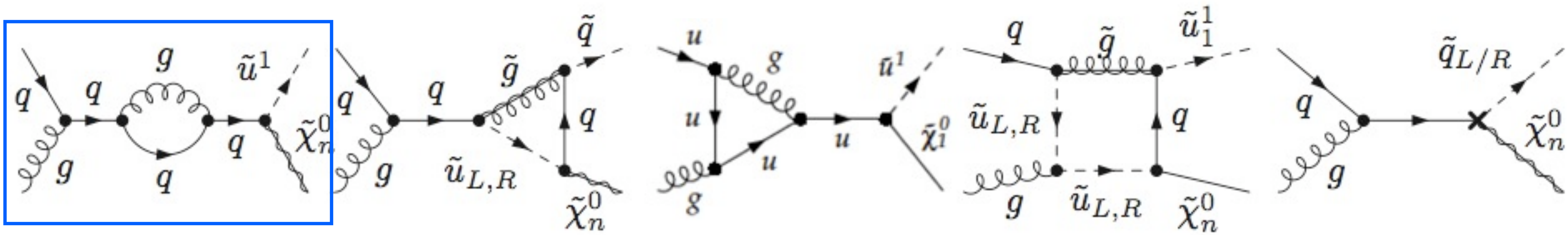

- a) self energy corrections; b) vertex corrections; c) box diagrams; d) UV counter terms

Structure of the NLO corrections

- **Virtual** QCD and SUSY-QCD corrections:

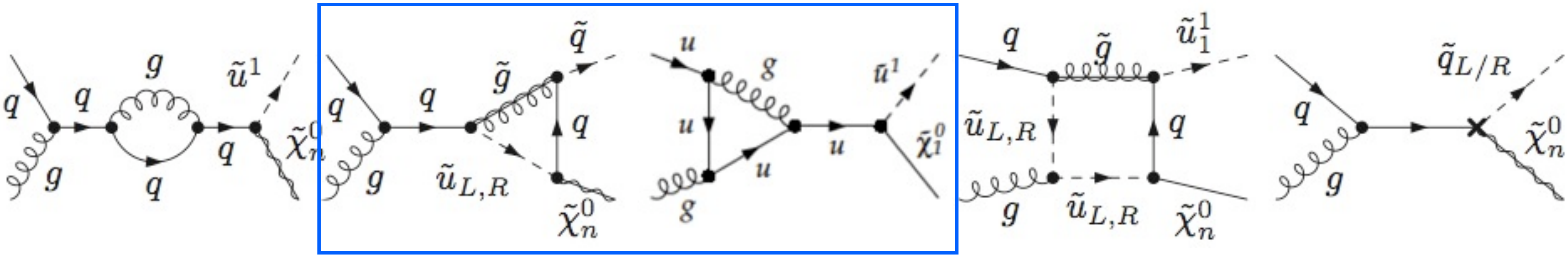

- a) self energy corrections; b) vertex corrections; c) box diagrams; d) UV counter terms

Structure of the NLO corrections

- **Virtual** QCD and SUSY-QCD corrections:

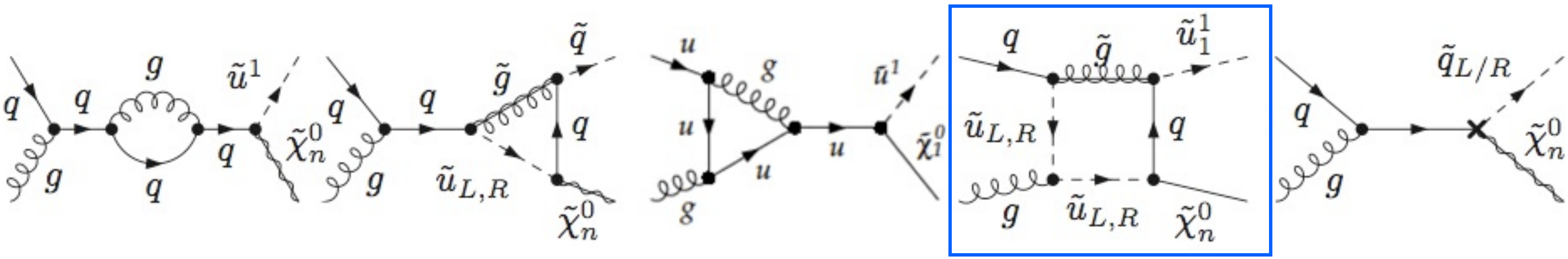

- a) self energy corrections; b) vertex corrections; c) box diagrams; d) UV counter terms

Structure of the NLO corrections

- **Virtual** QCD and SUSY-QCD corrections:

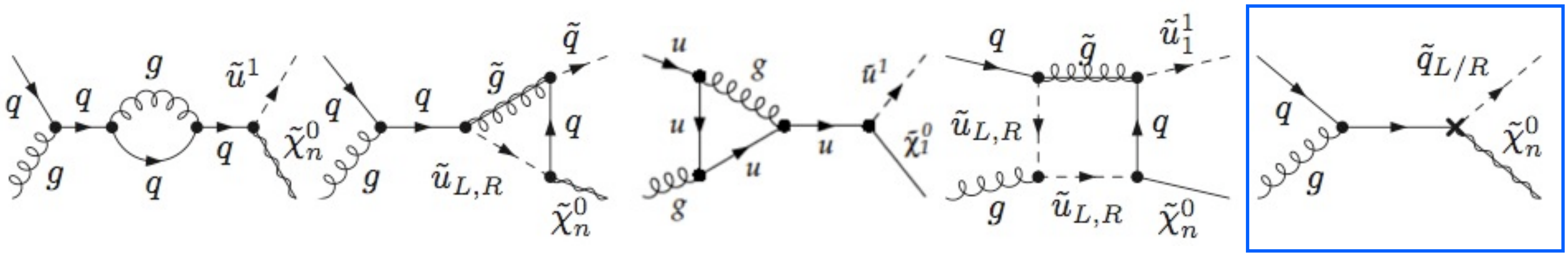

- a) self energy corrections; b) vertex corrections; c) box diagrams; d) UV counter terms

Structure of the NLO corrections

- **Virtual** QCD and SUSY-QCD corrections:

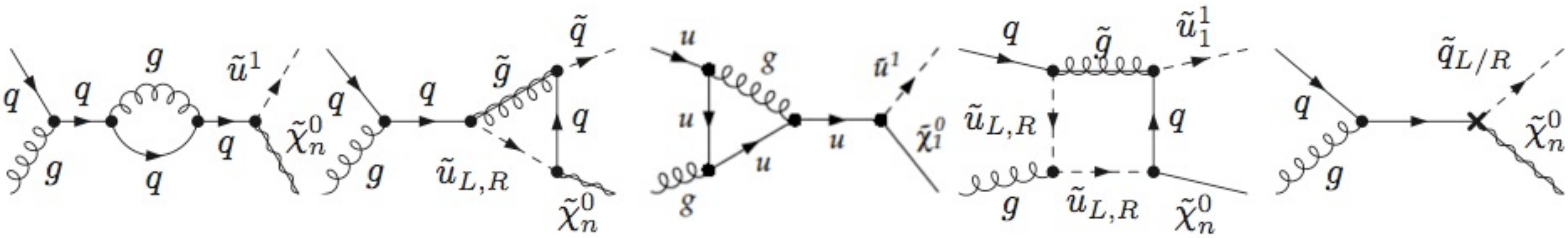

- a) self energy corrections; b) vertex corrections; c) box diagrams; d) UV counter terms

After all this have been automatically calculated, let's look at the physics results!

Scale Dependence

- Stabilization of the scale dependence on the unphysical μ_R & μ_F

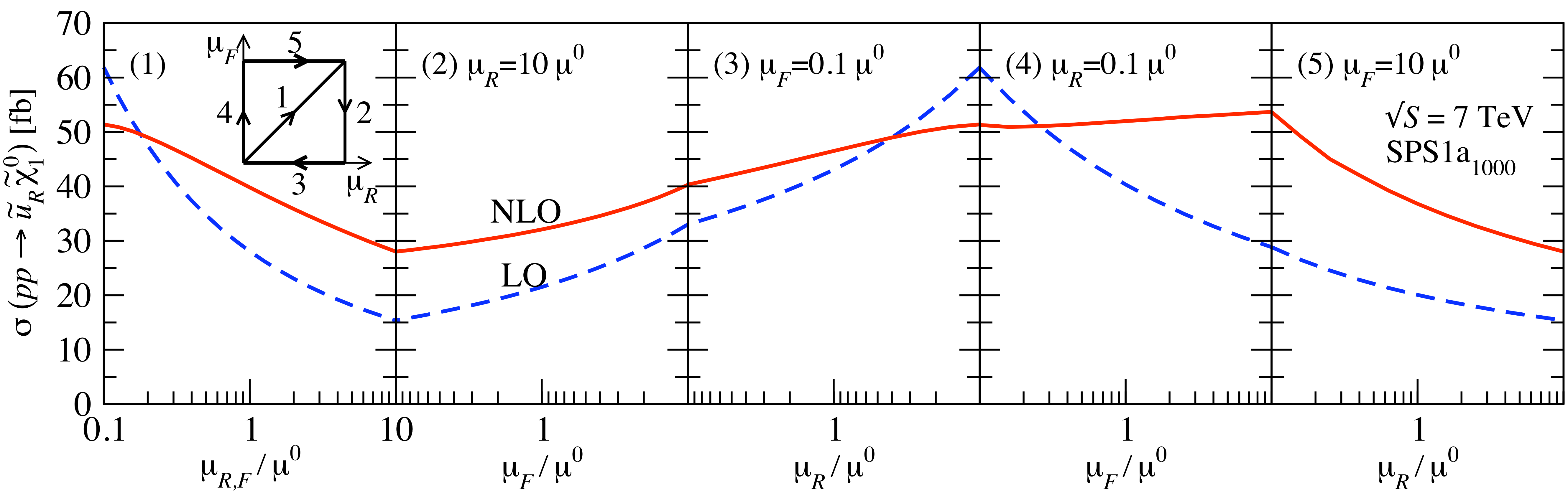

$\frac{\delta\sigma^{NLO}}{\sigma^{NLO}} \leq 20\%$, down from up to $\frac{\delta\sigma^{LO}}{\sigma^{LO}} \leq 70\%$

- Unlike Drell-Yan-type channels there is μ_R dependence at LO: $\sigma^{LO} \sim \alpha_s$

  But doesn't dominate completely the scale dependence as in QCD pair production

T. Binoth, DGN, D. Lopez-Val, T. Plehn, K. Mawatari, I. Wigmore [Phys. Rev. D84 (2011) 075005]

Scale Dependence

[Phys. Rev. D84 (2011) 075005]

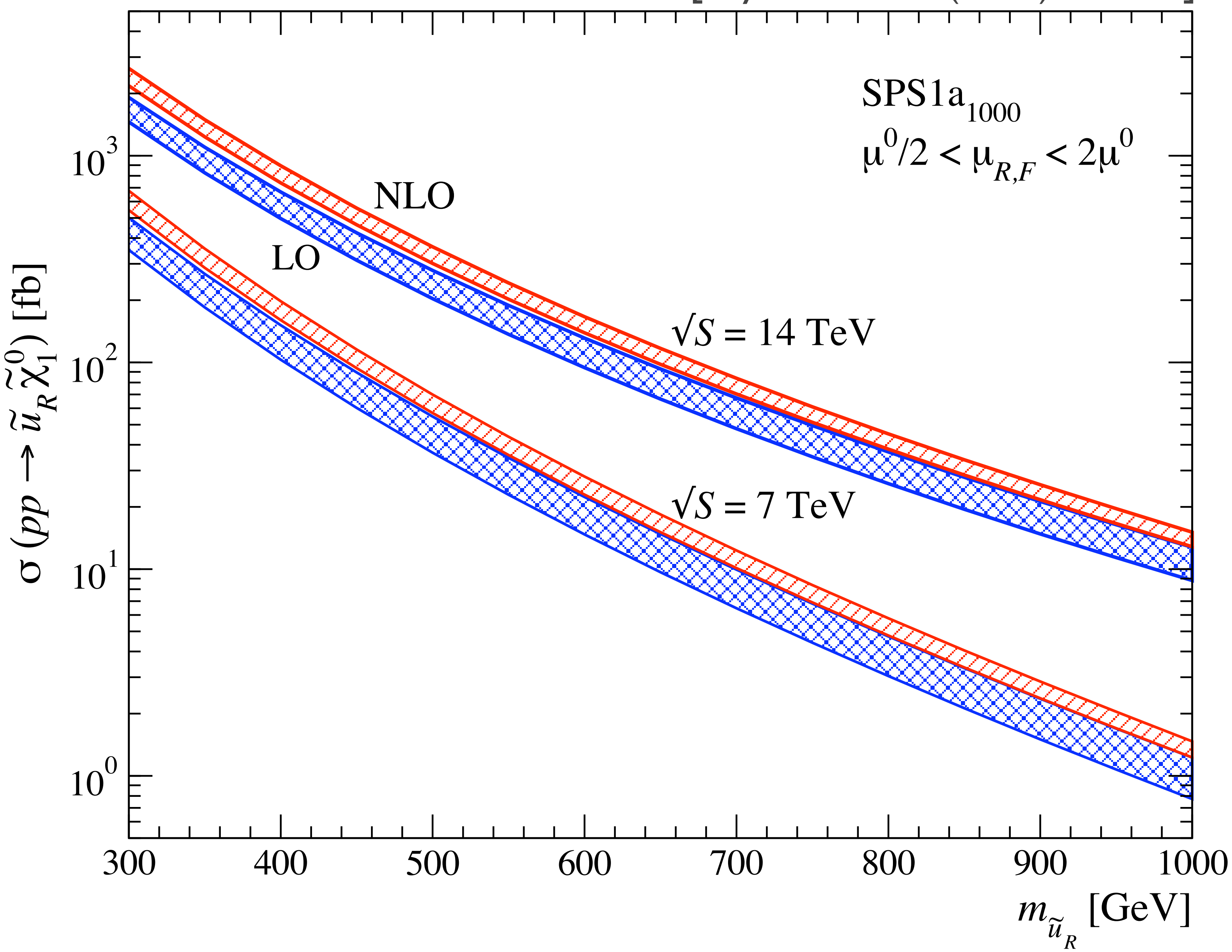

- Theory uncertainty largely reduced: $\frac{\delta\sigma^{NLO}}{\sigma^{NLO}} \leq 20\%$, down from up to $\frac{\delta\sigma^{LO}}{\sigma^{LO}} \leq 70\%$

Structure of the NLO corrections

[Phys. Rev. D84 (2011) 075005]

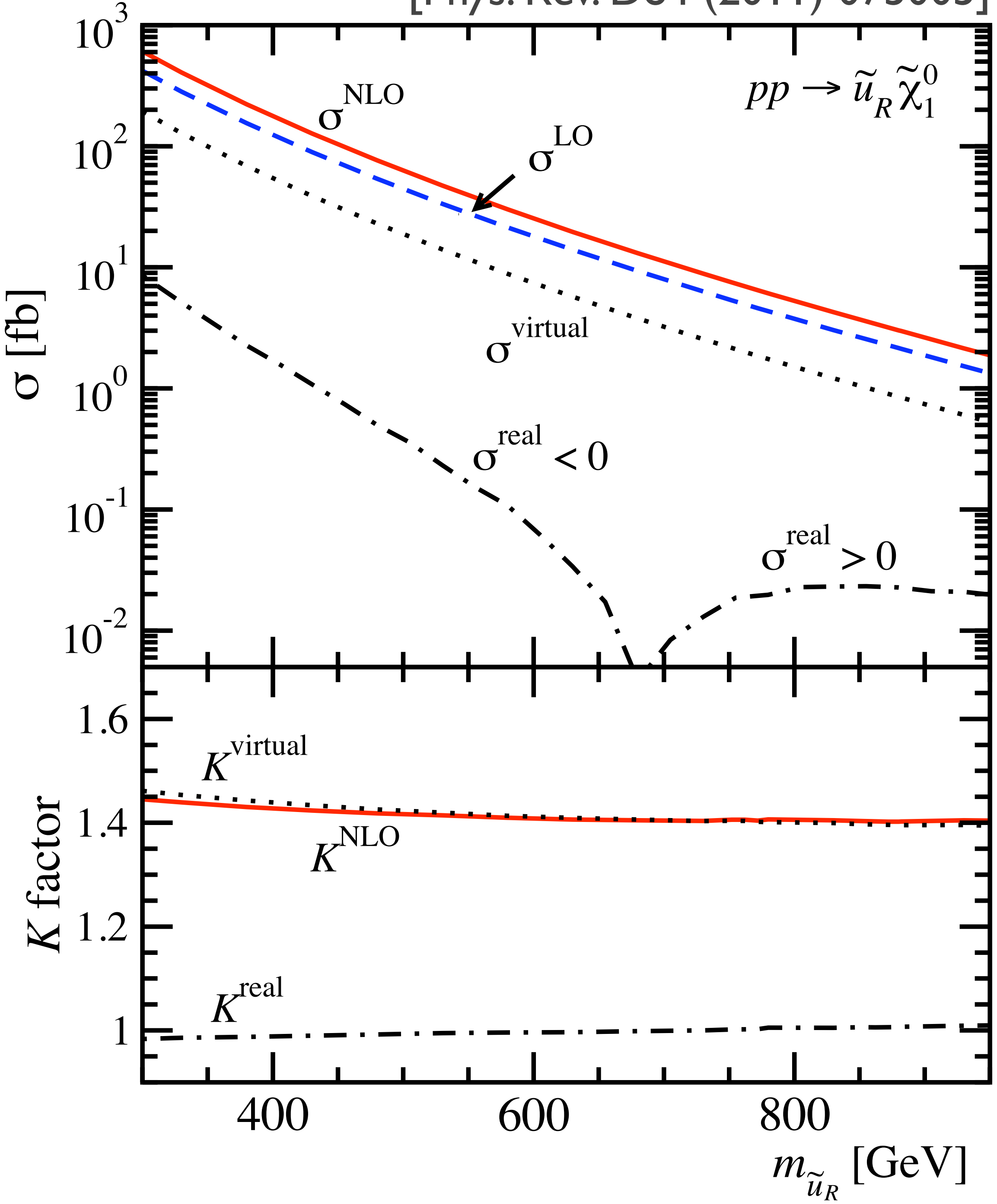

- $u\bar{u}g$ vertex correction basically independent on $m_{\tilde{u}}$
- SQCD effects have a subleading contribution supressed by $\frac{1}{M_{SUSY}}$

➡ Dominance by genuine QCD effects

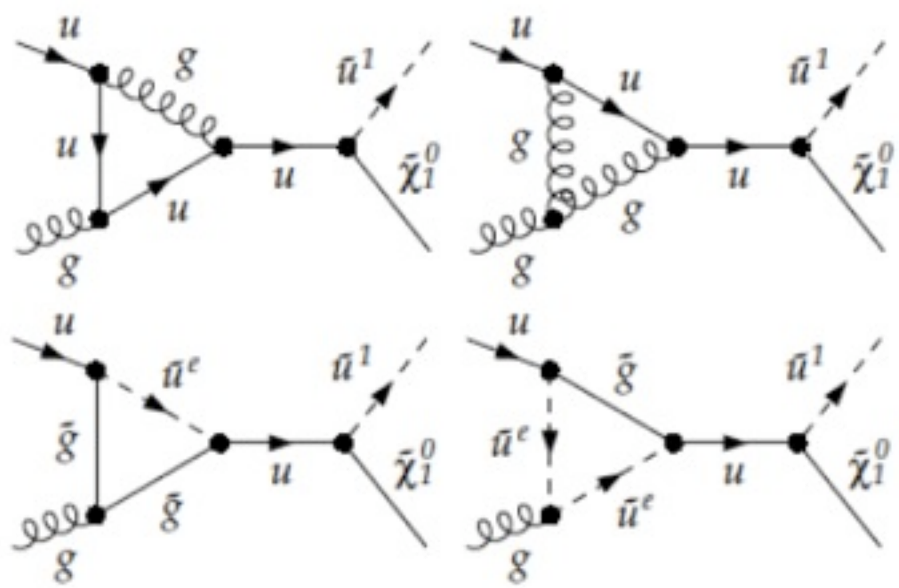

Structure of the NLO corrections

[Phys. Rev. D84 (2011) 075005]

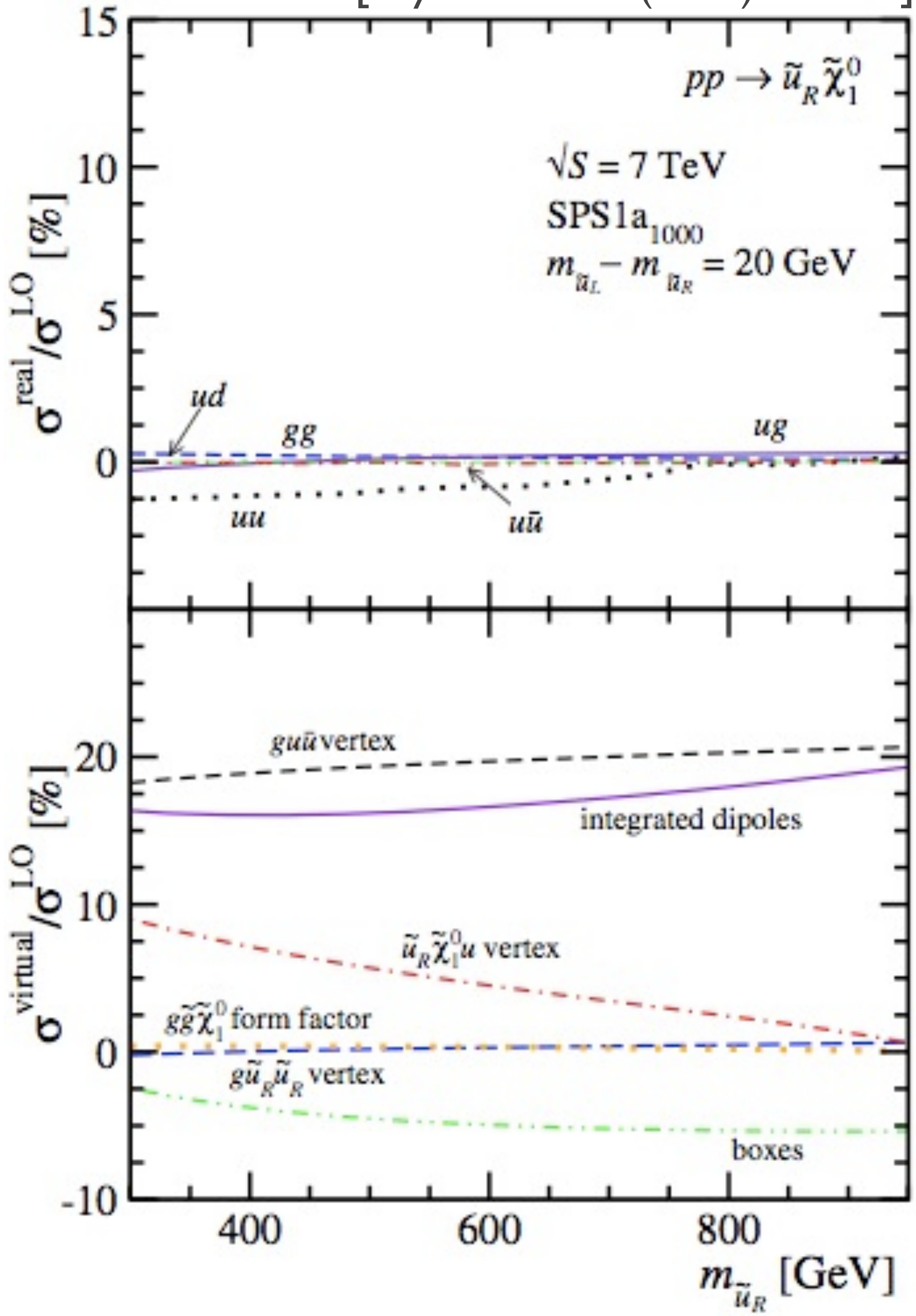

- $u\bar{u}g$ vertex correction basically independent on $m_{\tilde{u}}$
- SQCD effects have a subleading contribution supressed by $\frac{1}{M_{SUSY}}$

→ Dominance by genuine QCD effects

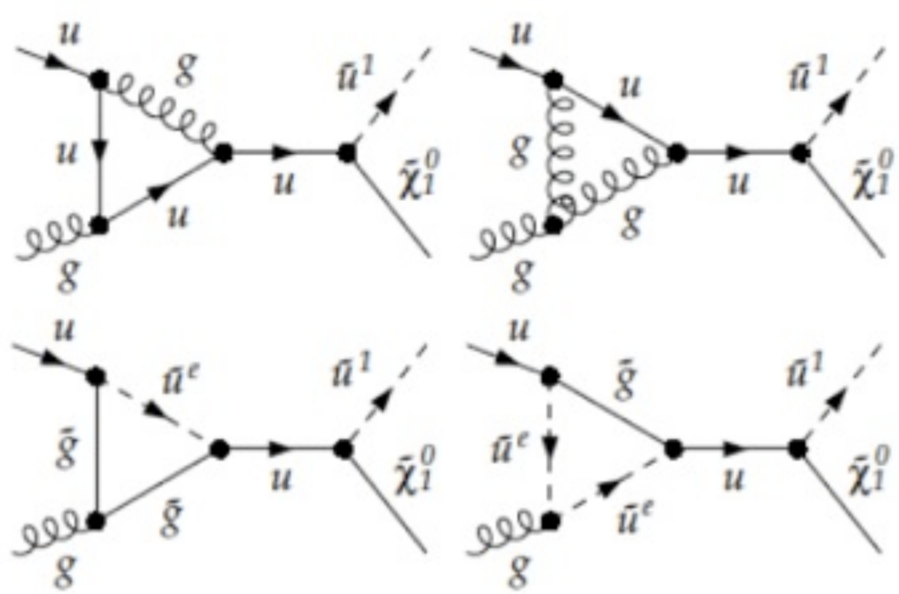

squark-gaugino channels

[Phys. Rev. D84 (2011) 075005]

$pp \to \tilde{q}\tilde{\chi}$

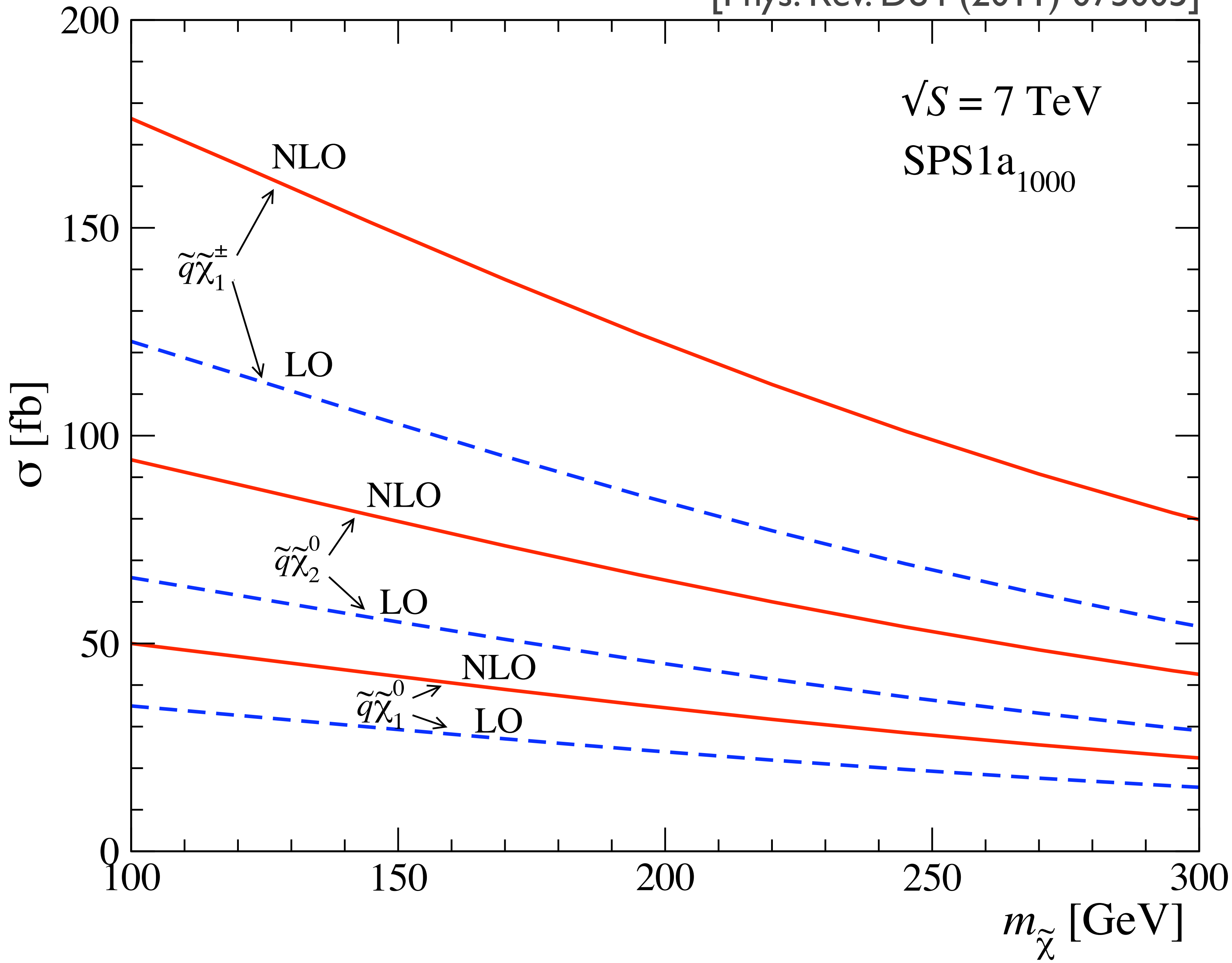

- Differences can be traced back to the size of the coupling $g_{q\tilde{q}\tilde{\chi}_1^0}$: $\left(\frac{g_{u\tilde{u}_L\tilde{\chi}_2^0}}{g_{u\tilde{u}_L\tilde{\chi}_1^0}}\right)^2 \sim 1.8$

Comparison with Multi-jet Merging

[Phys. Rev. D84 (2011) 075005]

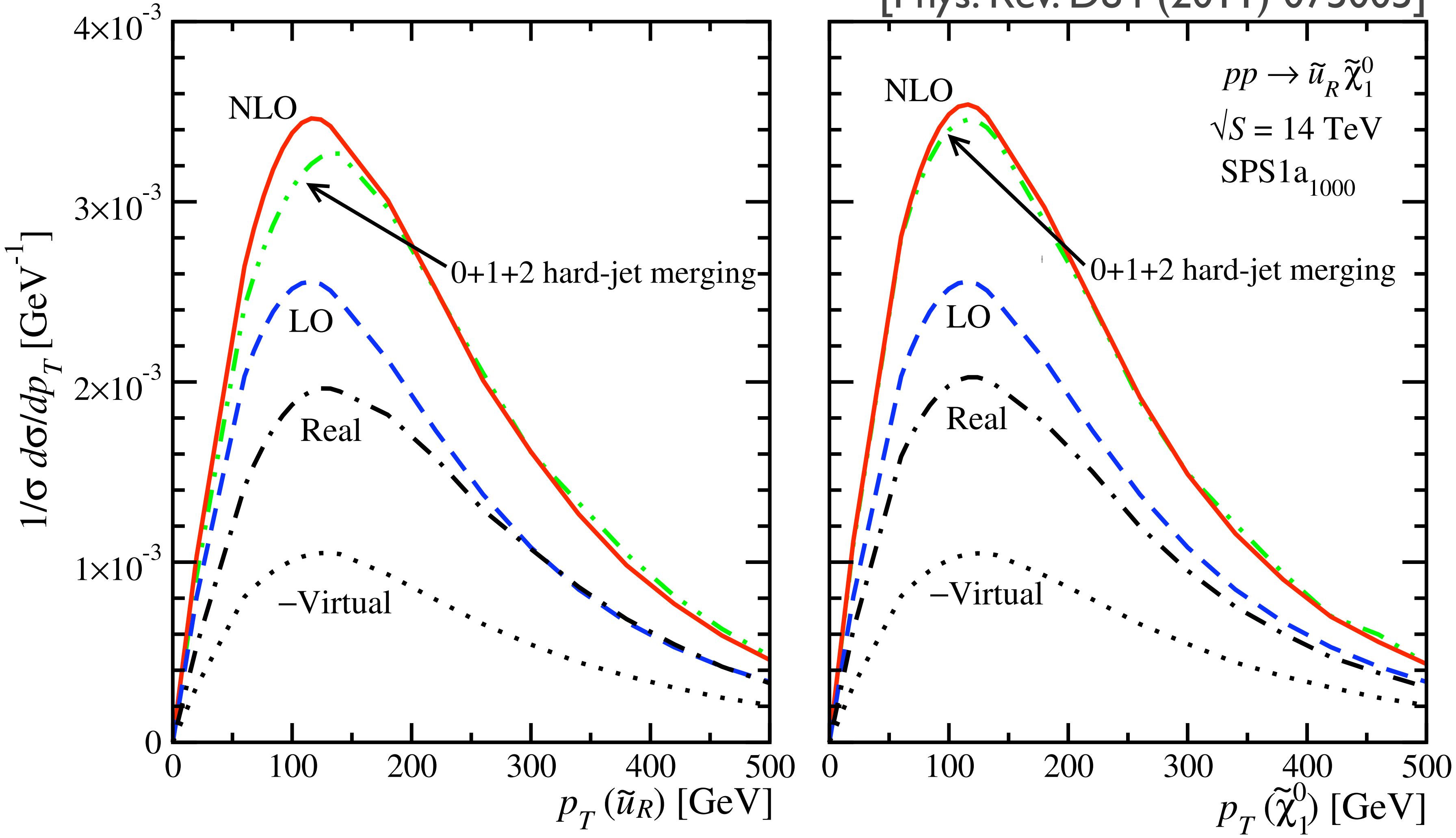

- Jet merging: combine ME + Parton Shower without double counting

  ME ↙ Partons are hard and well separated ↘

  Parton Shower ↘ Partons are soft/collinear (resums large logs) ↙

  Complementary

- NLO distributions for the heavy final states in good agreement with multi-jet merged calculation via MLM matching with MadGraph5.

Summary

- Structures of the NLO correction
- $pp \to \tilde{q}\tilde{\chi}_1^0$ @ NLO (First fully automized BSM NLO computation)
  - Source of mono-jets + $\not{E}_T$
  - Scale uncertainty largely reduced from 70% @LO to 20% @NLO
  - K factors largely insensitive to each SPS point
    Dominance from genuine QCD effects
  - High K for all SPS points K~1.4
  - NLO distributions in agreement with MLM matching

- Outlook: All SUSY pair production will be publicly available soon in MadGOLEM

MSSM parameter space

	$\sqrt{S}$ [TeV]	σ^{LO} [fb]	σ^{NLO} [fb]	K	$m_{\tilde{u}}$	$m_{\tilde{d}}$	$m_{\tilde{g}}$	$m_{\tilde{\chi}_1^0}$
SPS1a$_{1000}$	7	35.27	50.44	1.43	$\tilde{u}_L$: 561	$\tilde{d}_L$: 568	1000	97
	14	215.02	301.27	1.40	$\tilde{u}_R$: 549	$\tilde{d}_R$: 545		
SPS1b	7	2.77	3.99	1.45	$\tilde{u}_L$: 872	$\tilde{d}_L$: 878	938	162
	14	27.21	37.46	1.38	$\tilde{u}_R$: 850	$\tilde{d}_R$: 843		
SPS2	7	0.04	0.07	1.52	$\tilde{u}_L$: 1554	$\tilde{d}_L$: 1559	782	123
	14	1.21	1.64	1.36	$\tilde{u}_R$: 1554	$\tilde{d}_R$: 1552		
SPS3	7	3.15	4.55	1.44	$\tilde{u}_L$: 854	$\tilde{d}_L$: 860	935	161
	14	30.20	41.59	1.38	$\tilde{u}_R$: 832	$\tilde{d}_R$: 824		
SPS4	7	6.44	9.04	1.40	$\tilde{u}_L$: 760	$\tilde{d}_L$: 766	733	120
	14	52.87	71.40	1.35	$\tilde{u}_R$: 748	$\tilde{d}_R$: 743		
SPS5	7	13.26	18.11	1.37	$\tilde{u}_L$: 675	$\tilde{d}_L$: 678	722	120
	14	95.81	132.29	1.38	$\tilde{u}_R$: 657	$\tilde{d}_R$: 652		
SPS6	7	9.84	14.06	1.43	$\tilde{u}_L$: 670	$\tilde{d}_L$: 676	720	190
	14	77.08	107.03	1.39	$\tilde{u}_R$: 660	$\tilde{d}_R$: 650		
SPS7	7	2.19	3.17	1.45	$\tilde{u}_L$: 896	$\tilde{d}_L$: 904	950	163
	14	22.36	30.80	1.38	$\tilde{u}_R$: 875	$\tilde{d}_R$: 870		
SPS8	7	0.65	0.95	1.45	$\tilde{u}_L$: 1113	$\tilde{d}_L$: 1122	839	139
	14	8.73	11.79	1.35	$\tilde{u}_R$: 1077	$\tilde{d}_R$: 1072		
SPS9	7	0.39	0.58	1.49	$\tilde{u}_L$: 1276	$\tilde{d}_L$: 1279	1872	187
	14	7.65	10.42	1.36	$\tilde{u}_R$: 1282	$\tilde{d}_R$: 1289		

- Total cross section strongly depend on the SPS points:

a) **Kinematics**: dependence on the final state masses in phase space

b) **Dynamics**: coupling $g_{q\tilde{q}\tilde{\chi}_1^0}$ changes substantially for each scenario

- K factor largely insensitive to the specific SPS point: $K = \sigma^{NLO}/\sigma^{LO} \sim 1.4$

→ Dominance by genuine QCD effects

Backup slides

$\sqrt{S}$ [TeV]		$\sigma^{\rm LO}$ [fb]	$\sigma^{\rm NLO}$ [fb]	K		$\sigma^{\rm LO}$ [fb]	$\sigma^{\rm NLO}$ [fb]	K	$m_{\tilde{q}_R}$ [GeV]	$m_{\tilde{q}_L}$ [GeV]
7	$\tilde{u}_R\,\tilde{\chi}_1^0$	29.62	42.17	1.42	$\tilde{u}_L\,\tilde{\chi}_1^0$	0.83	1.26	1.52	549	561
14		176.36	245.74	1.39		5.03	7.52	1.49		
7	$\tilde{d}_R\,\tilde{\chi}_1^0$	3.61	5.31	1.47	$\tilde{d}_L\,\tilde{\chi}_1^0$	1.21	1.77	1.46	545	568
14		24.89	35.50	1.43		8.67	12.37	1.43		
7	$\tilde{c}_R\,\tilde{\chi}_1^0$	1.12	1.81	1.61	$\tilde{c}_L\,\tilde{\chi}_1^0$	0.03	0.06	2.00	549	561
14		13.69	20.69	1.51		0.38	0.66	1.70		
7	$\tilde{s}_R\,\tilde{\chi}_1^0$	0.57	0.78	1.38	$\tilde{s}_L\,\tilde{\chi}_1^0$	0.19	0.29	1.56	545	568
14		5.86	8.45	1.44		2.00	2.98	1.49		
7	$\sum \tilde{q}_R\,\tilde{\chi}_1^0$	34.92	50.07	1.43	$\sum \tilde{q}_L\,\tilde{\chi}_1^0$	2.26	3.38	1.50		
14		220.80	310.38	1.41		16.08	23.53	1.46		

- $SPS1a_{1000}$ has bino like neutralino $\left(\frac{g_{u\tilde{u}_L\tilde{\chi}_1^0}}{g_{u\tilde{u}_R\tilde{\chi}_1^0}}\right) \sim \frac{1}{6} \Rightarrow \sigma\left(\tilde{u}_R\tilde{\chi}_1^0\right) \gg \sigma\left(\tilde{u}_L\tilde{\chi}_1^0\right)$

Backup slides

$$\sigma^{Real}(\Gamma_{os}) = \int_{n+1} d\Phi_{n+1}\left[\left(|\mathcal{M}_{res}|^2 - d\sigma^{os}\right) + 2Re\left[\mathcal{M}^*_{res}\mathcal{M}_{rem}\right] + |\mathcal{M}_{rem}|^2 - d\sigma^A\right]$$

- gg>urn1ux

1 possible OS particle: ur

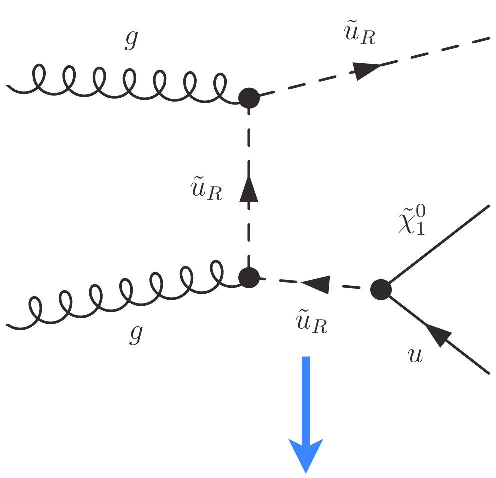

$$\frac{i}{p^2 - m_{OS}^2} \to \frac{i}{p^2 - m_{OS}^2 + i m_{OS}\Gamma_{OS}}$$

Γ_{OS} is a regulator!